Proceedings of the 25th International Conference on
Port and Ocean Engineering under Arctic Conditions
June 9-13, 2019, Delft, The Netherlands

Using Satellite observation data to estimate minimum design air temperatures distribution in Arctic

Yuanren Xiu, Zhijun Li, Qingkai Wang, Yongheng Zu, Peng Lu
State Key Laboratory of Coastal and Offshore Engineering, Dalian University of Technology, Dalian, China

ABSTRACT

For Arctic marine and coastal structures, such as ships and platforms, besides the need to withstand anticipated ice conditions, the ability to withstand the risk of low temperature is equally important. The designs of ocean and coastal structures in the Arctic low temperature region need to meet requirements of engineering design criteria and standards. The long-term time series of historical temperature is needed to satisfy requirements of these criteria and standards. In the past, estimating the minimum design temperature distributions in large-scale areas by only using the historical temperature data of very few ground meteorological stations in the corresponding areas was difficult to meet the accuracy requirements of ocean engineering applications. Because these ground meteorological stations are mostly distributed in the coastal land, the limitation of the station distribution and whether their temperature data can reasonably reflect the sea surface temperature have brought many uncertainties. Satellite observations are good means to obtain large-scale temporal and spatial meteorological data in the Arctic Ocean. In this paper product data downloaded from the NASA MERRA-2 reanalysis project are used to estimate the minimum design temperatures in the Arctic Ocean. Then, the contour maps of these design temperatures is drawn and an example is given to illustrate their practical application in engineering design. The influences of the changing trend of historical minimum temperature data on determining design temperatures are also discussed.

KEY WORDS: Arctic; Air temperatures; Design criteria and standards; Satellite data; Contour maps.

INTRODUCTION

Since the 21st century, the Arctic has warmed twice as fast as the global average. This phenomenon, widely known as the “Arctic Amplification Effect”, has led to the rapid melting of Arctic sea ice (Screen and Simmonds, 2010; Gao, et al., 2015; Serreze and Meier, 2019). Some research results predicted that there would be no ice in summer in the Arctic Ocean in the middle of this century (Liu, et al., 2013; Koenigk, et al., 2013).

The rapid melting of Arctic sea ice has undoubtedly brought unprecedented opportunities for Arctic shipping trade, resource development and polar scientific research. In particular, the opening of the Arctic Passage will bring huge economic benefits to all countries in the world (Ng, et al., 2018). In recent years, ocean engineering in the Arctic has become a hot topic of discussion and research, especially after the launch of the Yamal project. On July 19, 2018, the Yamal project supplied LNG to China via the Northeast Passage through the Bering Strait for the first time. Starting from the Russian port of Sabetta, this course travels east through the Kara Sea, the Laptev Sea, the East Siberian Sea, the Chukchi Sea to the Bering Strait, and then travels south to China via the Pacific Ocean, covering a distance of about 10,700 kilometers, saving about 13,400 kilometers compared with the conventional route through the Suez Canal, taking about 18 days on average, saving more than half a month compared with the traditional route through the Suez Canal, as shown in Fig. 1.

Image Source: www.eia.gov

Figure1. Yamal project LNG transportation routes

Based on the above backgrounds, the necessity of Arctic ocean engineering research is self-evident (Sulistiyono, et al., 2014). For Arctic ocean and coastal structures, such as ships and platform structures, besides the need to withstand the expected ice conditions, the ability to withstand low temperature risks is equally important. Low temperature environment will increase the operational difficulty of structures, weakening the performance of structures and pose a threat to the stability and safety of structures (Bridges, et al., 2018). Therefore, in order to ensure the efficient operation of structures, economic property safety and human life safety, the impact of low temperature environment can not be ignored.

The designs of marine and coastal structures in the Arctic low temperature region need to meet the requirements of engineering design criteria and standards. The determinations of design temperatures will affect the operation limitation, the selection of construction materials, the overall performance, the selection of auxiliary equipment and the implementation of emergency measures of polar ships and offshore platforms. Under these engineering design standards and criteria, the determinations of design temperatures should be based on the continuous time series of historical temperature data. In the past, it was difficult to satisfy the spatial accuracy requirements of ocean engineering designs by using only a few historical data of ground meteorological stations in the corresponding areas to evaluate the design temperatures of large-scale areas. Because these ground meteorological stations are mostly distributed in the coastal land, there are many uncertainties in the limitation of the station distribution and whether their temperature data can reasonably reflect the sea surface temperature. Satellite observations are effective means to obtain large-scale temporal and spatial meteorological data in the Arctic Ocean. In this paper, satellite product data are used to obtain the Arctic Ocean design temperature distributions. Then, the contour maps are drawn and an example analysis is provided to illustrate how the design temperature distributions are applied to engineering designs in the Arctic Ocean. Finally, the historical minimum temperature data of a location on the Northeast Passage are analyzed, and the influences of the changing trend on determining the design temperatures are discussed.

MERRA-2 AIR TEMPERATURE DATA

The Arctic Ocean temperature distribution dataset used in this paper is obtained from the temperature products of the National Aeronautics and Space Administration (NASA) MERRA-2 reanalysis project (Global Modeling and Assimilation Office (GMAO) (2015), MERRA-2 statD_2d_slv_Nx: 2d, Daily, Aggregated Statistics, Single-Level, Assimilation, Single-Level Diagnostics V5.12.4, Greenbelt, MD, USA, Goddard Earth Sciences Data and Information Services Center (GES DISC), Accessed: [2018-12-15], doi:10.5067/9SC1VNTWGWV3). MERRA-2 is a NASA atmospheric reanalysis for the satellite era using the Goddard Earth Observing System Model, Version 5 (GEOS-5) with its Atmospheric Data Assimilation System (ADAS), version 5.12.4 (Gelaro, et al., 2017). MERRA-2 reanalysis is widely used in Arctic research(Smith, et al., 2017; Rozenhaimer, et al., 2018). Although surface observations are rare in many parts of the Arctic, polar orbiting satellites cover this area widely, which has great advantages in obtaining large-scale surface temperature in the Arctic. Temperature products are one of the most reliable products in reanalysis products. The estimated surface air temperature obtained from the reanalysis was compared with the air temperature measured by ground stations (such as GISS-TEMP), and the result was satisfactory (Chung, et al., 2013).

MERRA-2 data files are provided in netCDF-4 format. The original dataset of temperature products adopts cubic spherical grids. For users convenience, the distributed dataset has been interpolated into the conventional longitude and latitude grid through bilinear space, and the spatial resolution is 0.625°×0.5° (Strobach, et al., 2018). The variables of air temperature products mainly include daily maximum air temperature, daily average air temperature and daily minimum air temperature at 2m above the surface. The products adopt thermodynamic temperature scale in the unit of K. The MERRA-2 data file provides user-defined downloads and are available from Jan. 1st, 1980 to the present (Shikwambana, 2019). The time span of product data used in this paper is from Dec. 1st, 1998 to Nov. 30th, 2018, totaling 20 years. The spatial scope of the product data downloaded covers the range of longitude -180° to 180°, latitude 60° to 90°.

DESIGN TEMPERATURE DEFINITIONS AND STATISTICAL METHODS

Before discussing the design temperature, we need to understand the following definitions of temperatures (Bridges, et al., 2018):

Mean Daily High Temperature, MDHT
Mean Daily Average Temperature, MDAT
Mean Daily Low Temperature, MDLT
Absolute Daily Minimum Temperature, ABSmin
Lowest Mean Daily Low Temperature, LMDLT
Lowest Mean Daily Average Temperature, LMDAT
Absolute Minimum Temperature, ABSMIN

Assuming that the time span of historical temperature series is N years (N≥10), these temperatures are expressed in the form of T_{ij}, which represents the temperatures of the ith day in the jth year and the subscripts min, max and mean are used to represent different statistical temperature values in one day:

$$\mathrm{MDHT_i} = \underset{1\le j\le N}{mean}\, T_{max_{ij}} \quad (1)$$

$$\mathrm{MDAT_i} = \underset{1\le j\le N}{mean}\, T_{mean_{ij}} \quad (2)$$

$$\mathrm{MDLT_i} = \underset{1\le j\le N}{mean}\, T_{min_{ij}} \quad (3)$$

$$\mathrm{ABS_{mini}} = \underset{1\le j\le N}{min}\, T_{min_{ij}} \quad (4)$$

Accordingly, there are:

$$\mathrm{LMDAT} = \underset{1\le i\le 366}{min}\, MDAT_i = \underset{1\le i\le 366}{min}\, \underset{1\le j\le N}{mean}\, T_{mean_{ij}} \quad (5)$$

$$\mathrm{LMDLT} = \underset{1\le i\le 366}{min}\, MDLT_i = \underset{1\le i\le 366}{min}\, \underset{1\le j\le N}{mean}\, T_{min_{ij}} \quad (6)$$

$$\mathrm{ABSMIN} = \underset{1\le i\le 366}{min}\, ABSmin_i = \underset{1\le i\le 366}{min}\, \underset{1\le j\le N}{min}\, T_{min_{ij}} \quad (7)$$

On the base of these, a variety of design criteria and standards for marine engineering in the Arctic region give many different design temperature definitions. It is clear that different methods are considered when determining the design temperatures. This paper mainly considers three design temperatures defined by IMO Polar Code (IMO, 2014), IACS UR S6 (IACS, 2018) and ISO 19906 (ISO, 2010).

IMO Polar Code is mainly applied to the polar ship. IMO Polar Code (Part I-A, 1.2.9) stipulates that the time span of historical temperature series used for statistical calculation of MDLT should not be less than 10 years. IMO Polar Code (Part I-A, 1.2.11-12) points out that the ships intending to operate in a low temperature environment means that the LMDLT of the area to be sailed or passed will be lower than -10℃, and for the expected operating area and season, the ship's Polar Service Temperature (PST) should be defined as at least 10℃ lower than LMDLT. IACS UR S6 is mainly applied to the polar ships. IACS UR S6.3 also stipulates that the time span of the historical temperature series used for statistics should not be less than 10 years, and defines that the design temperature t_D is equal to the LMDAT of the ship's operation area and should not be more than 13℃ higher than PST. ISO 19906 is mainly applied to offshore oil and gas structures in the Arctic. ISO 19906 (3.48) defines Lowest Anticipated Service Temperature (LAST) as minimum hourly average extreme level (EL) (annual probability of exceedance not greater than 10^{-2}) air temperature.

The datasets of daily maximum, average and minimum air temperatures were extracted from the downloaded MERRA-2 historical temperature products. After subtracting 273.15 from all the grid data values, the data were transformed into centigrade scale, and the unit was changed to ℃. The datasets of daily maximum, average and minimum air temperature of 2m above the surface were processed separately. All grid data of the distribution datasets of the same date in different years were averaged the number of years, and the series of 366-day MDHT, MDAT and MDLT distribution datasets in the Arctic Ocean were obtained. The datasets of daily minimum temperature of 2m above the surface were processed, minimizing each grid data with the same date for different years, and the series of 366-day ABSmin distribution datasets in the Arctic Ocean were obtained. Taking the grid data at Lat 70°N, Lon 180° as an example, taking the data at the position in the four distribution datasets series of MDHT, MDAT, MDLT, and ABSmin to form the process lines of these four variables for 366 days, and on this basis, the minimum values of the above four variables are taken as LMDHT, LMDAT, LMDLT, and ABSMIN, as shown in Fig. 2.

The LAST, an extreme level value with an annual probability of exceedance not greater than 10^{-2}, is applied to offshore oil and gas platforms, which can be estimated by probability distribution. In this paper, the P-III probability distribution commonly used in engineering is used to estimate LAST (Wu, et al., 2017). The minimum daily air temperature distribution datasets of 2m above the surface were processed, obtaining the annual absolute minimum value of each grid and then the 20-year annual ABSMIN distribution datasets series in the Arctic Ocean is obtained.

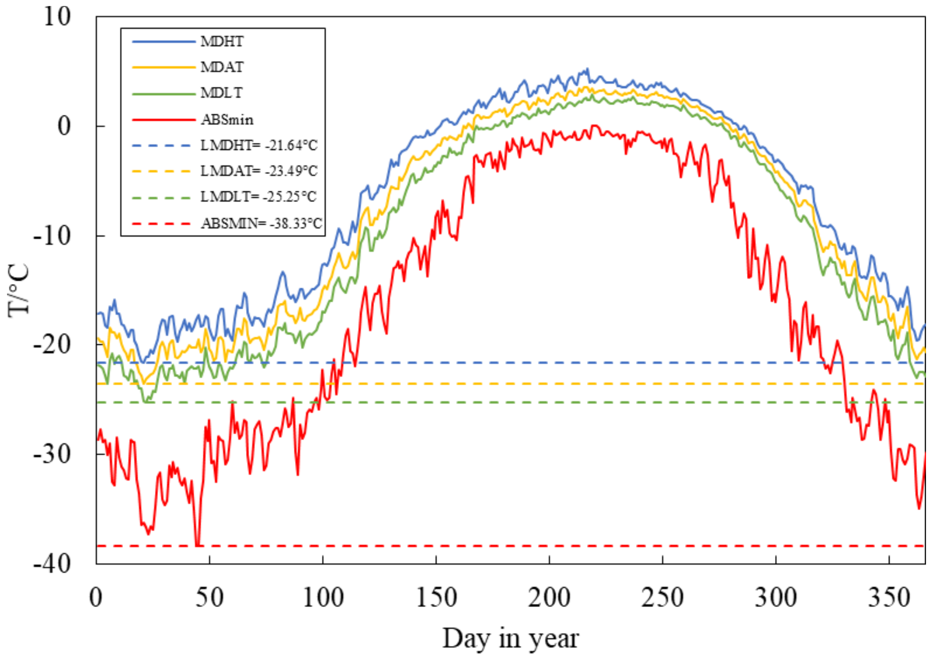

Figure 2. Time series diagram of different statistical daily temperatures results at Lat 70°N, Lon 180°

The P-III probability density curve is an asymmetric single peak and positive skew curve with one end finite and one end infinite. It is mathematically called gamma distribution. Its probability density function is as follows:

$$f(x) = \frac{\beta^{\alpha}}{\Gamma(\alpha)}(x - a_0)^{\alpha-1}e^{-\beta(x-a_0)} \tag{8}$$

In eq. (8), $\Gamma(\alpha)$ is a Gamma function, $\alpha > 0,\ \beta > 0$.
The design value x_P of the corresponding frequency P can be determined by Eq. (9):

$$x_P = K_P\bar{x} \tag{9}$$

$\bar{x}$ is the sample mean in eq. (9).

The frequency factor Φ_P and modular ratio coefficient K_P can be determined by Eq. (10) and Eq. (11):

$$\Phi_P = \frac{C_s}{2}t_P - \frac{2}{C_s} \tag{10}$$

$$K_P = \Phi_P C_v + 1 \tag{11}$$

In Eq. (10) and (11), C_v is the sample coefficient of deviation and C_s is the sample coefficient of skewness.

The value of the standard Gamma distribution quantile t_P can be calculated by Excel's built-in function GAMMAIN:

$$t_P = GAMMAINV(1 - P, \alpha, 1) \tag{12}$$

By plugging t_P into Eq. (10), the frequency factor Φ_P can be obtained, and then the modulus ratio coefficient K_P and the corresponding design value x_P can be obtained.

However, in the actual calculation process, it is found that the annual ABSMIN data series often presents negative skewness, in other words, its skewness coefficient C_s<0. At this time, the traditional P-III positive skewness equation has a large deviation in calculation. Therefore, the P-III negative skewness equation should be used instead.

If the probability density function of positive skewness distribution is f(x) and the probability density function of negative skewness distribution is g(x), according to the principle that the two probability density curves are symmetrical about the line through the mean value, when mean, deviation coefficient are equal and the skewness coefficient is opposite to each other, $f(x)$ and $g(x)$ are symmetrical about $x = \bar{x}$, i.e. $g(x) = f(2\bar{x} - x)$, then:

$$x_P = 2\bar{x} - GAMMAINV\left(P, \alpha, \frac{1}{\beta}\right) - a_0 \tag{13}$$

in which $\beta = \frac{2}{\bar{x}C_v|C_s|}$ and $a_0 = \bar{x}(1 - \frac{2C_v}{|C_s|})$. See Li and Zheng (2010) for details.
Therefore, in the statistical process of annual ABSMIN data series, different equations should be selected according to the different situations of C_s.

RESULTS AND DISCUSSIONS

The yearly minimum temperature data should be used as the basic data for determining the design temperatures for polar ships expected to sail in low temperature environment of the Arctic Ocean all year round. Distribution datasets of LMDAT (t_D), PST and ABSMIN in the Arctic Ocean can be obtained according to the above definitions and methods. Using these datasets, contour maps of the three yearly design temperatures in the Arctic Ocean can be drawn, respectively, as shown in Fig. 3. For polar ships expected to sail in the Arctic Ocean only in the time of higher temperature and lighter ice condition, if the yearly minimum temperature is used to make statistics, it will cause unnecessary waste in the selection of materials and auxiliary equipment in the process of ship design and construction. Therefore, the design temperature can be estimated by monthly temperature data, and for seasonally restricted service according to IACS UR S6 (IACS, 2018, Section S6.3), the design temperature t_D should be the lowest recorded value during operation (ABSMIN in the corresponding period). The distribution datasets and contour maps of PST and ABSMIN (t_D) in the Arctic Ocean corresponding to 12 months can be obtained respectively, as shown in Fig 4.

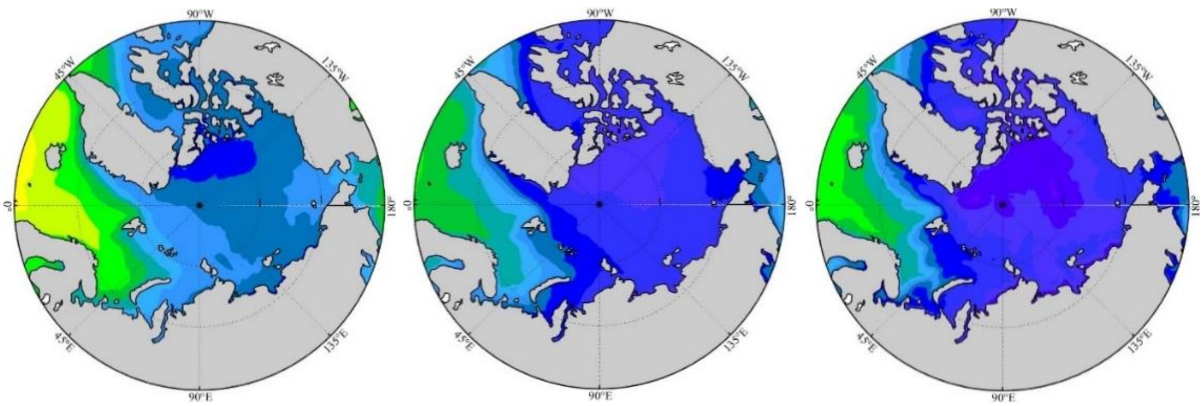

(a) (b) (c)

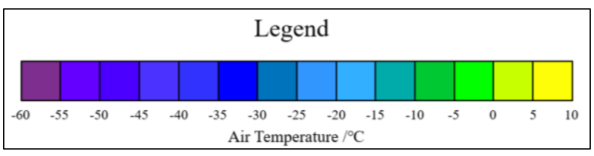

Figure 3. Contour maps of the three yearly design temperatures in the Arctic Ocean (a- LMDAT(t_D), b- PST, c- ABSMIN)

As can be seen from Fig. 3, for the yearly design temperatures, the lowest design temperature is distributed in the central parts of the Arctic Ocean on the northern side of Greenland and the Canadian Arctic Archipelago and in the narrow waters of Russia's Siberian coast, the highest design temperature is distributed in the Norwegian Sea, and the temperature gradient from the central parts to the Atlantic side of the Arctic Ocean is much larger than the temperature gradient to the Pacific side. This is roughly consistent with the distribution of Arctic sea ice thickness. The low design temperature in the Russian Siberian coastal waters is mainly due to its proximity to the Siberian inland, which has been occupied by the Siberian cold high pressure for a long time in winter, making this area a cold pole in the northern hemisphere.

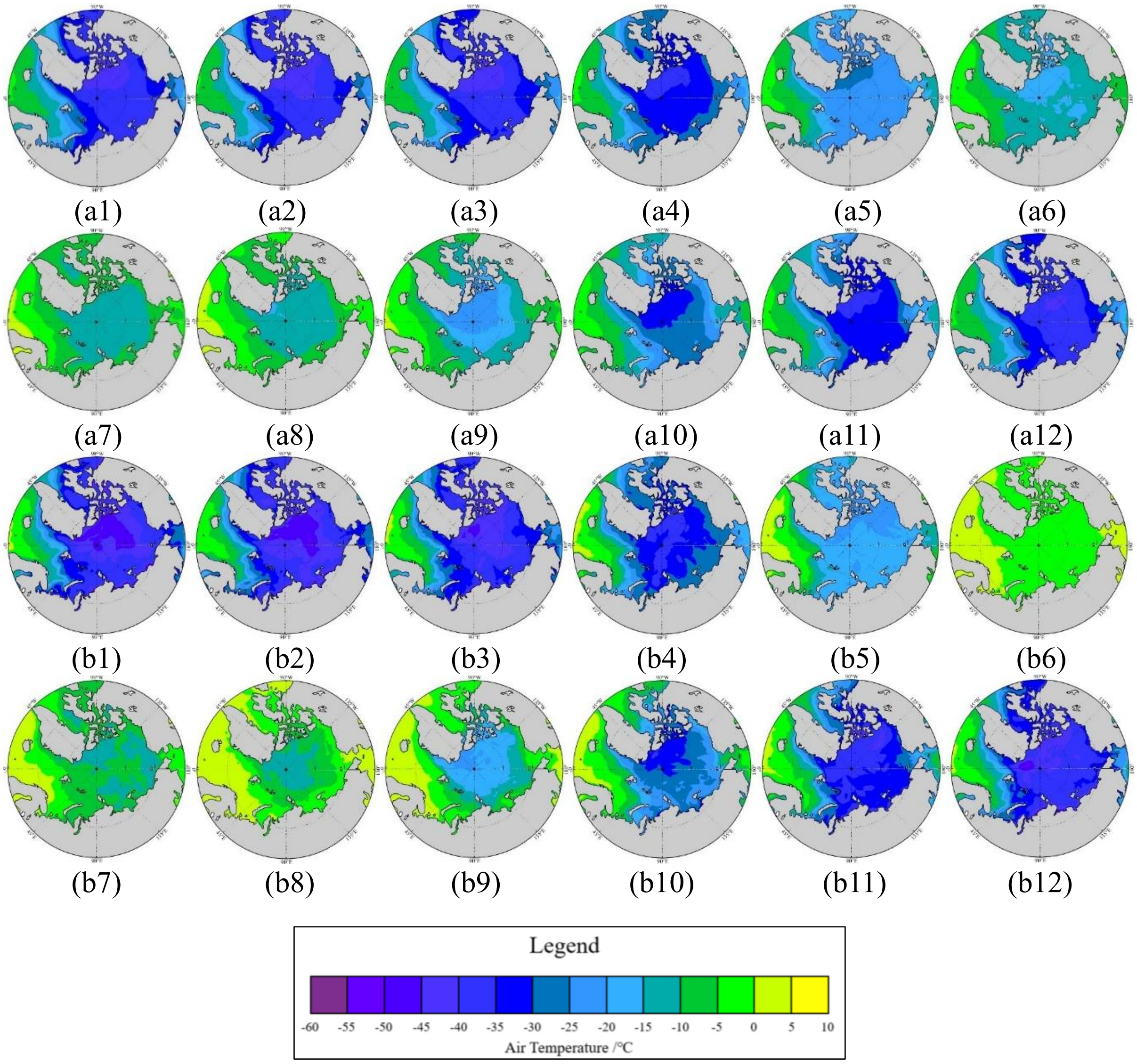

Figure 4. Contour maps of the two monthly design temperatures in the Arctic Ocean (a- PST, b- ABSMIN(t_D), 1- 12 represents January- December)

As can be seen from Fig. 4, for the 12-month design temperatures, the design temperatures of the Arctic Ocean reach the lowest level in February. In July, the design temperatures in the central Arctic Ocean reach the highest level in the whole year, and in August, the design temperatures in the marginal Arctic Ocean reach the highest level in the whole year. Overall, the Norwegian Sea maintains the highest design temperature throughout the year, and its yearly temperature difference of each design temperature is very small.

Frequency has abstract mathematical meaning. If the occurrence of an event can not be predicted, only through a large number of measured data, the probability of occurrence can be estimated by mathematical statistics method. This probability is called empirical frequency. Frequency is often replaced by return period in engineering. The return period is the average interval between occurrences of a situation that the design value greater than or equal to a specified value, using year (a) as the unit. The return period is inversely proportional to the frequency, i.e. T=1/P. Therefore, the return period corresponding to the extreme level value of LAST which represents an annual exceedance probability of no greater than 10^{-2} is 100 years. 20-year time sequence values of each grid are statistically analyzed by P-III probability distribution, and probability distribution curves of ABSMIN can be obtained, from which ABSMIN with a return period of 100 years, i.e. LAST can be extracted. In this way, the LAST distribution dataset can be obtained and contour map of the Arctic Ocean can be drawn, as shown in Fig. 5. It should be pointed out here that the data used for statistical calculation of LAST is the daily minimum temperature dataset rather than the hourly average temperature dataset, so LAST obtained here will be lower, but for marine engineering, the applications of this result in design will be safer.

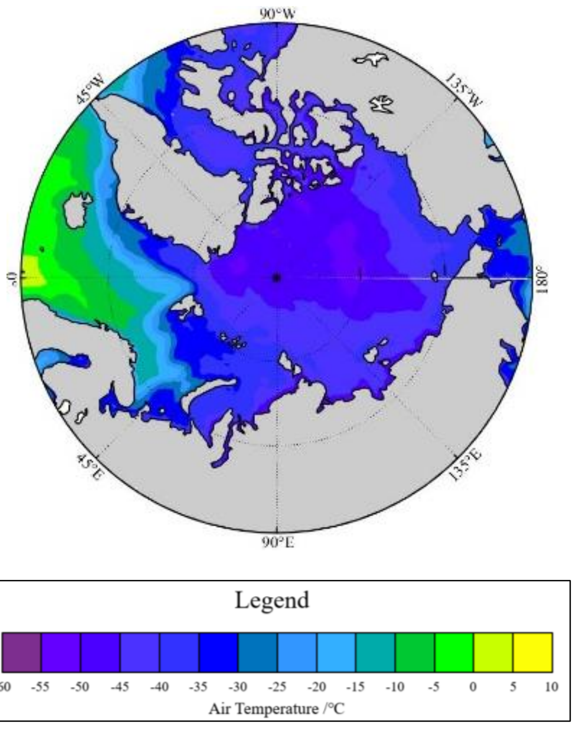

Figure 5. Contour map of LAST in the Arctic Ocean

The following is an example to illustrate the applications of design temperature contour maps in engineering. Assuming that the LNG vessel of the Yamal Project sails from Sabetta to the Bering Strait along the Northeast Passage and then sails southward into the Pacific Ocean, part of its route north of 60°N is shown in the red line in Fig. 6. Considering the ice condition of this route, assuming that this route only opens from July to October every year, the lowest design temperatures in the area of this route during July to October can be selected as the key design parameters in the design stages of the ship. According to Fig. 6, the lowest ABSMIN (t_D)in this route area during July- October is between –25°C and 30°C. According to the safety design principle of “Choosing low value instead of high value” in anti-low temperature designs, the design temperature t_D of the ship is determined to be -30°C. The method of IACS UR S6 estimating t_D in material application has been accepted by many industries (Sulistiyono, et al., 2014 & 2015). According to IACS UR S6, steel grades for different classes of structural materials can be determined, as shown in Table 1.

Temperature data at Lat 70°N, Lon 180° are still used as analysis objects. See Fig. 6 for the location. From 1999 to 2018, LAST of each period is estimated in turn every continuous 10 years. The results are shown in Fig. 7. The corresponding annual ABSMIN of 1999- 2018 is also shown in Fig. 7. As can be seen from Fig. 7, ABSMIN at this location have increased in the past 20 years, correspondingly, LAST shows the same trend, which is consistent with the current trend of global warming. The estimation of LAST is mainly influenced by the annual lowest temperature ABSMIN. It can be seen that with the increase of annual ABSMIN, LAST enlarges the trend of this increase, and the rate of rise of LAST is more than twice that of ABSMIN. Because the annual mean of ABSMIN is used in LAST estimation, the upward trend is more stable. The above shows that under the background of global warming, the design temperatures estimated from the historical daily temperature data would be higher. Assuming that global warming continues to develop, the statistical results of design temperatures will also maintain this upward trend, which will lower many requirements and limits in the design and construction of ships expected to sail in the Arctic Ocean.

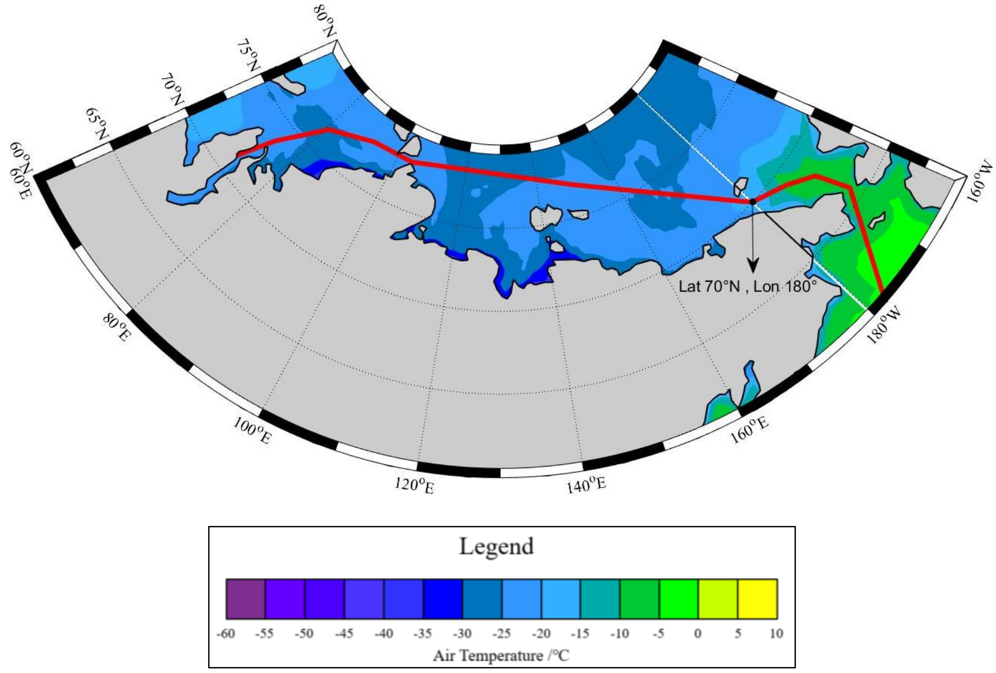

Figure 6. Contour map of ABSMIN in July to October in the area around the assumed route

Table 1. Steel Grade Requirements for Material Classes I, II and III at -30°C in IACS UR S6

<table>
<tr><th>Plate thickness, in mm</th><th>Material Class I</th><th>Material Class II</th><th>Material Class III</th></tr>
<tr><td>t⩽10</td><td>B</td><td>D</td><td>D</td></tr>
<tr><td>10<t⩽15</td><td>D</td><td rowspan="2">D</td><td rowspan="2">E</td></tr>
<tr><td>15<t≤20</td><td>D</td></tr>
<tr><td>20<t≤25</td><td>D</td><td rowspan="2">E</td><td>E</td></tr>
<tr><td>25<t≤30</td><td>D</td><td>E</td></tr>
<tr><td>30<t≤35</td><td>D</td><td rowspan="2">E</td><td>Not applicable</td></tr>
<tr><td>35<t≤40</td><td rowspan="2">E</td><td>Not applicable</td></tr>
<tr><td>40<t≤45</td><td>Not applicable</td><td rowspan="2">Not applicable</td></tr>
<tr><td>45<t≤50</td><td>E</td><td>Not applicable</td></tr>
</table>

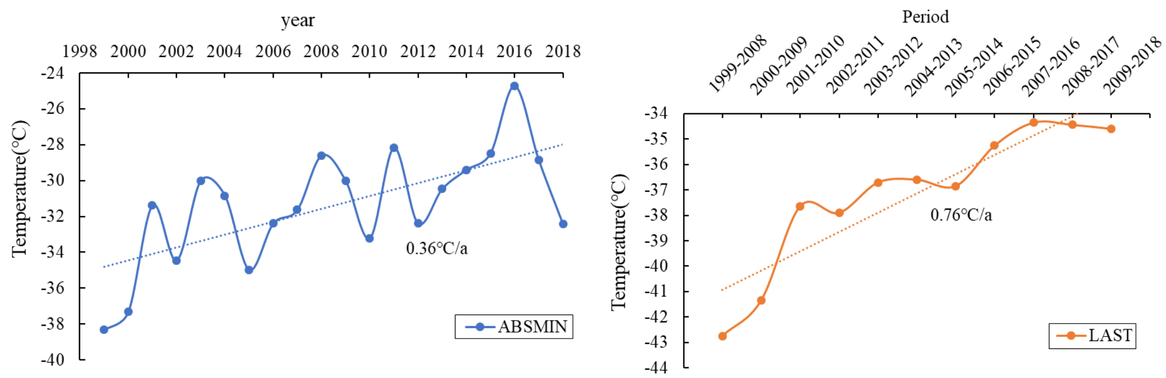

Figure 7. Changes of ABSMIN and LAST in 1999-2018 at Lat 70°N, Lon 180°

CONCLUSIONS

It is very important to know the design temperature distributions of the Arctic Ocean for ships and offshore platform structures expected to operate in the Arctic Ocean. For the anti-low temperature designs of polar ships and offshore platform structures, the engineering design criteria require using the long-term historical temperature data series. The daily temperature products of the MERRA-2 reanalysis project were downloaded from NASA from Dec. 1st, 1998 to Nov. 30th, 2018, from which the daily maximum, average and minimum temperature data in the Arctic Ocean were extracted.

According to the design temperature definitions of IMO Polar Code, IACS UR S6 and ISO 19906, the distribution datasets of LMDAT(t_D), PST and ABSMIN in the Arctic Ocean were obtained. Correspondingly, using these datasets, the contour maps of the three yearly design temperatures in the Arctic Ocean were drawn. Considering polar ships only expected to navigate seasonally in the low-temperature regions of Arctic Ocean, using monthly temperature data, the distribution datasets of PST and ABSMINN (t_D) in the Arctic Ocean corresponding to 12 months were obtained and the contour maps were drawn. The LAST distribution dataset of the Arctic Ocean was obtained and the contour map of LAST in the Arctic Ocean is drawn by using the P-III probability distribution which is commonly used in engineering. An example analysis is provided to illustrate how the Arctic Ocean design temperature distributions are applied to engineering design.

For the yearly design temperatures, the lowest design temperatures are located in the central Arctic Ocean on the northern side of Greenland and the Canadian Arctic Islands and in the narrow waters along the Siberian coast of Russia, the highest design temperature is located in the Arctic Ocean near the Atlantic Ocean. The temperature gradient from the central Arctic Ocean to the Atlantic Ocean is larger than that to the Pacific Ocean. For the monthly design temperatures in the Arctic Ocean, they reached the lowest level in February. In July, the design temperatures in the central sea area of the Arctic Ocean reached the highest level, and in August, the design temperatures in the marginal sea area of the Arctic Ocean reached the highest level. Overall, the Arctic Ocean near the Atlantic side maintains the highest design temperature throughout the year, and its annual temperature difference of each design temperature is small.

Taking the data at Lat 70°N, Lon 180° as the object of analysis. From 1999 to 2018, LAST of each period is estimated in turn every 10 continuous years and its change trend is compared with that of ABSMIN in 1999- 2018. The results show that under the background of global warming, the design temperatures calculated from historical daily temperature data would be higher.

ACKNOWLEDGEMENTS

We thank the GES-DISC of NASA for providing the MERRA-2 data. The MERRA-2 data is obtained online from https://disc.gsfc.nasa.gov/datasets/M2SDNXSLV_V5.12.4/summary. This research was funded by the Global Change Research Program of China (2015CB953901).

REFERENCES

Bridges, R., Riska, K., Lu, L., et al., 2018. A study on the specification of minimum design air temperature for ships and offshore structures. *Ocean Engineering*, 160, pp.478-489.

Chung, C.E., Cha, H., Vihma, T., et al., 2013. On the possibilities to use atmospheric reanalyses to evaluate the warming structure in the Arctic. *Atmospheric Chemistry and Physics*, 13(22), pp.11209-11219.

Gao, Y.Q., Sun, J.Q., Li, F., et al., 2015. Arctic sea ice and Eurasian climate: A review. *Advances in Atmospheric Sciences*, 32(1), pp.92-114.

Gelaro, R., McCarty, W., Suarez, M.J., et al., 2017. The Modern-Era Retrospective Analysis for Research and Applications, Version 2 (MERRA-2). *Journal of Climate*, 30(14), pp.5419-5454.

International Association of Classification Societies (IACS), 2018. *Use of Steel Grades for Various Hull Members - Ships of 90m in Length and above, UR, S6*, London: IACS.

International Maritime Organization (IMO), 2014. *International Code for Ships Operating in Polar Waters (Polar Code)*, London: IMO.

International Organization for Standardization (ISO), 2010. *Petroleum and Natural Gas Industries - Arctic Offshore Structures, ISO 19906*, Geneva: ISO.

Koenigk, T., Brodeau, L., Graversen, R.G., et al., 2013. Arctic climate change in 21st century CMIP5 simulations with EC-Earth. *Climate Dynamics*, 40(11-12), pp.2719-2743.

Li, X., and Zheng, J., 2010. A Brief Discussion on the Calculating Method of P-III Negative Bias Frequency Curve, *Guangdong Water Resources and Hydropower*, (9), pp.17-18.

Liu, J., Song, M., Horton, R.M., et al., 2013. Reducing spread in climate model projections of a September ice-free Arctic. *Proceedings of the National Academy of Sciences*, 110(31), pp.12571-12576.

Ng, A.K.Y., Andrews, J., Babb, D., et al., 2018. Implications of climate change for shipping: Opening the Arctic seas. *Wiley Interdisciplinary Reviews-Climate Change*, 9(2), pp.UNSP e507.

Rozenhaimer, M.S., Barton, N., Redemann, J., et al., 2018. Bias and Sensitivity of Boundary Layer Clouds and Surface Radiative Fluxes in MERRA-2 and Airborne Observations Over the Beaufort Sea During the ARISE Campaign. *Journal of Geophysical Research-Atmospheres*, 123(12), pp.6565-6580.

Screen, J.A., Simmonds, I., 2000. The central role of diminishing sea ice in recent Arctic temperature amplification. *Nature*, 464(7293), pp.1334-1337.

Serreze, M.C., Meier, W.N., 2019. The Arctic's sea ice cover: trends, variability, predictability, and comparisons to the Antarctic. *Annals of the New York Academy of Sciences*, 1436(1), pp.36-53.

Shikwambana, L., 2019. Long-term observation of global black carbon, organic carbon and smoke using CALIPSO and MERRA-2 data. *Remote Sensing Letters*, 10(4), pp.373-380.

Smith, L.C., Yang, K., Pitcher, L.H., et al., 2017. Direct measurements of meltwater runoff on the Greenland ice sheet surface. *Proceedings of the National Academy of Sciences of the United States of America*, 114, pp.E10622–E10631.

Strobach, E., Molod, A., Forget, G., et al., 2018. Consequences of different air-sea feedbacks on ocean using MITgcm and MERRA-2 forcing: Implications for coupled data assimilation systems. *Ocean Modelling*, 132, pp.91-111.

Sulistiyono, H., Lye, L.M., Khan, F.I., et al., 2014. Estimating Design Temperatures in Arctic Environments: A New Approach. In: *Proceedings of the Oceans/IEEE Conference*, St. John's, Newfoundland, 5 pp.

Sulistiyono, H., Khan, F.I., Lye, L.M., et al., 2015. A risk-based approach to developing design temperatures for vessels operating in low temperature environments. *Ocean Engineering*, 108, pp.813-819.

Wu, S., Feng A., Gao J, et al., 2017. Shortening the Recurrence Periods of Extreme Water Levels under Future Sea-level Rise. *Stochastic Environmental Research and Risk Assessment*, 31(10), pp.2573-2584.